Seismic Response and Damage Detection Analyses of an Instrumented Steel Moment-Framed Building

Janise E. Rodgers, M.ASCE[1]; and Mehmet Çelebi, M.ASCE[2]

Abstract: The seismic performance of steel moment-framed buildings has been of particular interest since brittle fractures were discovered at the beam–column connections in a number of buildings following the M 6.7 Northridge earthquake of January 17, 1994. A case study of the seismic behavior of an extensively instrumented 13-story steel moment frame building located in the greater Los Angeles area of California is described herein. Response studies using frequency domain, joint time–frequency, system identification, and simple damage detection analyses are performed using an extensive strong motion dataset dating from 1971 to the present, supported by engineering drawings and results of postearthquake inspections. These studies show that the building's response is more complex than would be expected from its highly symmetrical geometry. The response is characterized by low damping in the fundamental mode, larger accelerations in the middle and lower stories than at the roof and base, extended periods of vibration after the cessation of strong input shaking, beating in the response, elliptical particle motion, and significant torsion during strong shaking at the top of the concrete piers which extend from the basement to the second floor. The analyses conducted indicate that the response of the structure was elastic in all recorded earthquakes to date, including Northridge. Also, several simple damage detection methods employed did not indicate any structural damage or connection fractures. The combination of a large, real structure and low instrumentation density precluded the application of many recently proposed advanced damage detection methods in this case study. Overall, however, the findings of this study are consistent with the limited code-compliant postearthquake intrusive inspections conducted after the Northridge earthquake, which found no connection fractures or other structural damage.

DOI: 10.1061/(ASCE)0733-9445(2006)132:10(1543)

CE Database subject headings: Earthquakes; Earthquake engineering; Spectral analysis; Buildings, office; Seismic effects; Steel frames; Structural behavior.

Introduction

The Alhambra building is a 13-story office building located approximately 8 km east-northeast of downtown Los Angeles, and has a perimeter moment-resisting frame structural system. The building was designed in 1969 according to the 1967 Uniform Building Code, hereafter UBC (ICBO 1967), constructed in 1970, and instrumented in 1971 according to UBC recommendations for larger buildings (one triaxial accelerograph per floor at basement, midheight, and roof levels). Earthquakes for which the building's response has been recorded, along with magnitude and distance information, are shown in Fig. 1. Ambient vibration data (Dunand et al. 2004), engineering drawings, and results of postearthquake inspections (Black and Veatch, unpublished report, 1997) are also available.

Since the building has been strongly shaken by several earthquakes and has a substantial amount of data and supporting information available, it was chosen for a case study exploring its seismic response and attempting to determine if structural damage had occurred in any of the recorded earthquakes. Results presented herein are excerpted from a larger study of the building's seismic response that utilized the entire data set (Rodgers et al. 2004). Response summary data are presented for the strong motion recordings. The building's response to the Northridge earthquake is examined in detail using frequency domain, joint time–frequency, and system identification analyses. In addition, several simple damage detection methods are applied to the available data. The objectives of these studies are to investigate the possibility of structural damage and to gain understanding of the unexpectedly complex building response evident in the many strong motion recordings available for the building, as well as to illustrate some of the challenges involved in attempting to detect damage in a large, sparsely instrumented structure.

Background

Prior Studies on Alhambra Building

Several previous studies have examined aspects of the seismic response of the Alhambra building by several means, including: nonlinear dynamic analyses of a computer model of the building (Cohen 1996), evaluation of a single modal analysis-based damage detection method (Sanli and Çelebi 2002), and system identification (Goel and Chopra 1997; Çelebi, unpublished; Sanli and

[1]Project Manager, GeoHazards International, 200 Town and Country Village, Palo Alto, CA 94301 (corresponding author). E-mail: janise.rodgers@gmail.com

[2]Manager, Structural Monitoring, U.S. Geological Survey, MS977, 345 Middlefield Rd., Menlo Park, CA 94025.

Note. Associate Editor: Ahmet Emin Aktan. Discussion open until March 1, 2007. Separate discussions must be submitted for individual papers. To extend the closing date by one month, a written request must be filed with the ASCE Managing Editor. The manuscript for this paper was submitted for review and possible publication on October 15, 2004; approved on October 10, 2005. This paper is part of the *Journal of Structural Engineering*, Vol. 132, No. 10, October 1, 2006. ©ASCE, ISSN 0733-9445/2006/10-1543–1552/$25.00.

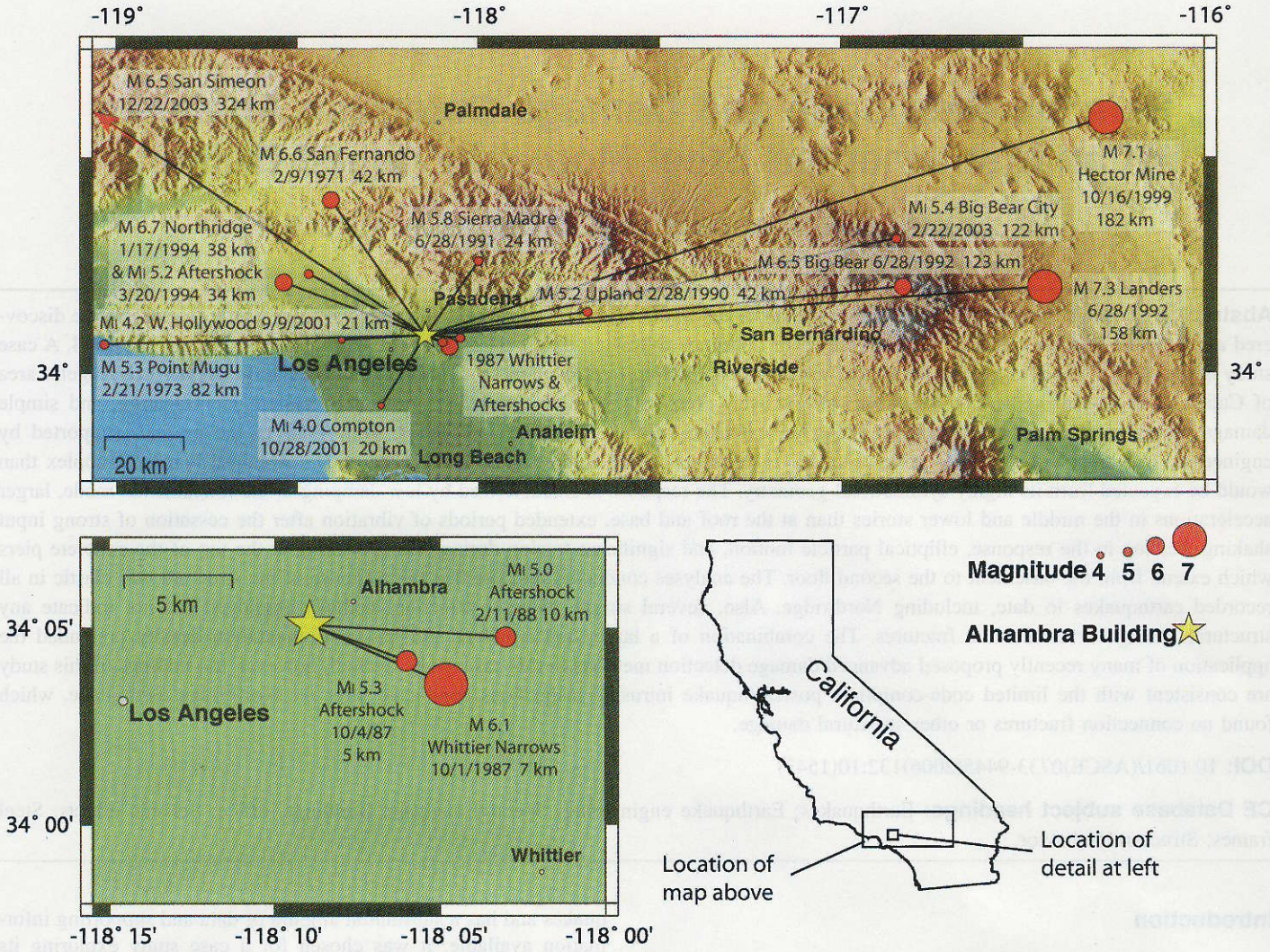

Fig. 1. (Color) Location of Alhambra building and epicenters of earthquakes with strong-motion data recorded

Çelebi 2002). However, each of these prior studies utilized data from only a few earthquakes, rather than the full 16-earthquake dataset used in the present study described herein.

Despite this, the previous investigations provided some valuable insights into the seismic response of the building in several of the recorded earthquakes. Based on the results of dynamic analysis, Cohen (1996) concluded that the building response was essentially elastic for the M 6.6 1971 San Fernando and the M 6.1 1987 Whittier Narrows earthquakes. Stiffness degradation of approximately 10% was deemed to occur in both directions (Sanli and Çelebi 2002) between the Whittier Narrows and M 7.1 1999 Hector Mine earthquakes. The source of this stiffness loss was not determined by the modal analysis-based damage detection method used, although it was attributed to minor structural and nonstructural damage caused by the Northridge earthquake.

Several interesting aspects of the behavior of the building were also noted by prior investigators. These aspects include prolonged response after the cessation of strong motion input (Cohen 1996; Sanli and Çelebi 2002), very low damping (Cohen 1996; Goel and Chopra 1997), beating (Sanli and Çelebi 2002), a tendency for the highest recorded accelerations to occur at intermediate floors rather than the roof (Cohen 1996; Sanli and Çelebi 2002), and difficulty in determining the second mode frequency due to the presence of several peaks on a swollen baseline in the Fourier amplitude spectra (Sanli and Çelebi 2002). These aspects of the building's behavior, along with several others, were observed in the course of the present study as well, and will be discussed in subsequent sections.

Damage Detection and System Identification Methods

A number of methods for damage detection in structures have been proposed recently (see Sohn et al. 2003 for a comprehensive review of current literature). Such methods include those based on the updating of finite-element (FE) models (e.g., Papadimitriou et al. 1997; Lopez-Diaz et al. 2000), neural networks (e.g., Nakamura et al. 1998; Masri et al. 2000), genetic algorithms, (e.g., Ruatolo and Surace 1998), wavelets (e.g., Hou et al. 2000; Kim and Melhem 2003), and mode shapes or mode shape derivatives (e.g., Doebling and Farrar 1997; Maeck and De Roeck 1999; Stubbs et al. 1999), among others. While many of these approaches are promising, practical limitations are encountered when trying to apply many of these methods to large, sparsely instrumented buildings such as the Alhambra building. In particular, methods that require a detailed and highly accurate three-dimensional FE model are impractical for this building, due to large computational demands and difficulties involved in obtaining the FE model. Despite its regular geometry, the building pre-

sents a number of modeling challenges, including approximately 1,000 fracture-capable moment-resisting beam-to-column connections, very stiff concrete piers, and a suspended mezzanine, in addition to nonstructural components and cladding. Some techniques are available (e.g., Fritzen and Boehle 1999a,b) for reducing the computations necessary with these methods, but do not remove the need for a detailed FE model, so this approach is not pursued in this study.

Neural network approaches do not explicitly require a detailed FE model, but do typically require a large number of data sets from various damage scenarios in order to train the network. For most real buildings, including the Alhambra building, the required quantity of data is not available from experimental sources (such as recordings during earthquake events). Data sets, typically those involving damage, must therefore be simulated and a FE model capable of accurately modeling damage is again required.

Due to the very low spatial resolution of the sensor network, damage detection methods based on mode shapes are not appropriate, and no attempt is made to identify mode shapes during system identification. Due to the numerous limitations posed by the structure and its sensor network, simple damage detection methods are utilized herein, with the exception of wavelets, which do not require FE models and can be used in cases with sparse instrumentation.

As is the case with damage detection, there have been numerous recent advances in system identification. A number of these are output-only models such as frequency domain decomposition (Brinker et al. 2000) and stochastic subspace identification (Van Overschee and De Moor 1993), which were developed with applications such as the analysis of ambient vibration data in mind. However, since a strong input signal is available for the seismic excitations examined herein, output-only techniques are not utilized. Rather, more classical system identification techniques are utilized herein, and are described in the section on system identification analyses. The analysis of the ambient vibration data available for the building, for which output-only methods would be used, lies outside the scope of this paper and is reported elsewhere (Dunand 2005).

Building Description

Structural System

The lateral force-resisting system of the Alhambra building consists of perimeter welded steel moment frames (WSMFs) above the second floor, and massive reinforced concrete piers below the second floor. The floor plan is square (50.5 m × 50.5 m), with floor framing consisting of lightweight concrete over metal decking without shear studs. Typical floor height and column spacing are 4.3 m (14 ft) and 4.6 m (15 ft), respectively. The perimeter moment frames are constructed of built up wide flange sections and are nominally identical in both directions except for the connections at the corner columns, which are pinned in the east-west (*E-W*) direction. In addition, there are several small moment frames in the *E-W* direction in the interior core. The moment frames were not designed in accordance with drift limits or strong column–weak beam criteria as the 1967 UBC did not contain these provisions. However, the design base shear computed using the 1967 UBC was multiplied by three as a means of drift control (Cohen 1996).

Typical perimeter moment frame beam sizes range from 30PG109 [meaning a 30 in. (760 mm) deep plate girder weighing

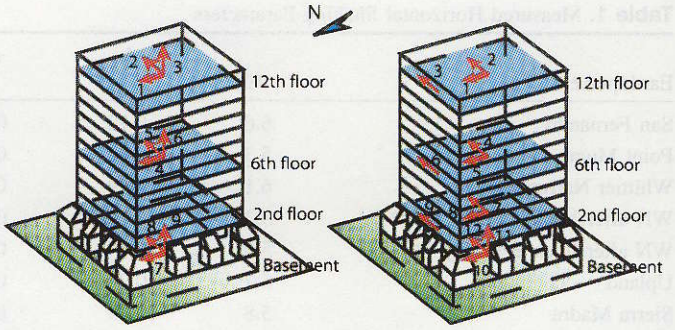

Fig. 2. (Color) Code-recommended (left) and extensive (right) instrumentation configurations

109 lb (0.485 kN) per linear foot] at the third floor to 24PG45 at the roof. Built up columns are 430 mm (17 in.) deep, and have flanges 200 mm (8 in.) wide. Perimeter moment frames are constructed of A36 steel, while interior frames are A572, with F_y=66 ksi (0.455 GPa) specified on the construction drawings. The moment frame columns are embedded 1.52 m (5 ft) into the piers, though the pier-to-column connections appear to have been designed for shear only. Large plate girders (57PG201) at the top of the piers transfer loads from noncontinuous perimeter columns. The perimeter moment connections differ in two ways from the standard pre-Northridge detail: (1) the web was welded rather than bolted; and (2) vertical column flange stiffeners were used instead of continuity plates.

The massive two-story reinforced concrete piers that extend from the ground floor to the second floor are significantly stiffer than the moment frame, despite their height (see Fig. 2). The piers are constructed integrally with concrete columns which extend from the ground floor through the basement to the foundation. Further information on the structural system can be found in Cohen (1996).

Instrumentation

Fig. 2 shows the evolution of the seismic instrumentation schemes in the Alhambra building. The building was initially instrumented in early 1971 according to UBC recommendations mandated by the County of Los Angeles. Triaxial accelerometers were installed at three levels: the basement, sixth, and 12th floors. The instrumentation was improved to a 12-channel structural array in 1989. The sensors used in the array were three uniaxial force balance accelerometers (FBAs) per floor at the second, sixth, and 12th floors, and a triaxial accelerometer in the basement. The FBAs at the second, sixth, and 12th floors were deployed in a manner permitting both translational and torsional measurements. In 1996 a digital recorder replaced the analog recorder, and in 1998 a triaxial instrument was deployed in the free field on the building grounds.

Building Performance in Past Earthquakes

The two earthquakes with the strongest measured shaking at the Alhambra building, and thus with the most damage potential, were the Whittier Narrows and Northridge earthquakes. Following the Northridge earthquake, ultrasonic testing (UT) by both the county and a private consultant (Black and Veatch, unpublished report, 1997) detected weld defects or small cracks with FEMA designation W1 or W5 (FEMA 1995) in 30 of the 52 inspected

Table 1. Measured Horizontal Shaking Parameters

Earthquake	M	A_{bo} (g)	A_{12o} (g)	A_{so} (g)	Level and direction of A_{so}	D_{bo} (cm)	D_{12o} (cm)
San Fernando	6.6	0.12	0.18	0.18	12-EW	7.7	19.3
Point Mugu	5.3	0.02	0.02	0.03	6-NS	0.2	0.7
Whittier Narrows (WN)	6.1	0.29	0.27	0.47	6-EW	2.4	7.5
WN aftershock October 14,1987	5.3[a]	0.14	0.18	0.24	6-EW	0.5	1.7
WN aftershock February 11,1988	5.0[a]	0.04	0.03	0.05	6-EW	0.1	0.2
Upland	5.2	0.02	0.03	0.05	2-EW	0.3	1.9
Sierra Madre	5.8	0.13	0.15	0.28	2-EW	1.8	6.5
Landers	7.3	0.03	0.12	0.12	12-EW	7.5	13.3
Big Bear	6.5	0.02	0.06	0.06	12-NS	1.1	5.0
Northridge (NR)	6.7	0.16	0.14	0.54	2-EW	1.7	12.4
NR aftershock March 20,1994	5.2[a]	0.03	0.02	0.09	2-NS	0.1	0.5
Hector Mine	7.1	0.04	0.10	0.10	12-EW	12.2	16.9
West Hollywood	4.2[a]	0.02	0.008	0.05	2-NS	<0.1	0.2
Compton	4.0[a]	0.008	0.003	0.02	2-NS	<0.1	<0.1
Big Bear City	5.3[a]	0.004	0.006	0.01	2-NS	<0.1	0.1
San Simeon	6.5	0.004	0.03	0.03	12-EW	0.6	3.2

[a]Denotes local magnitude; moment magnitude used otherwise.

moment connections (an inspection rate of ~5%). No other structural damage was found, though some nonstructural damage was noted. The connections were reinspected using UT with backing bars removed, and core samples from select locations were examined under a microscope, revealing slag inclusions and zones of incomplete fusion, both indicators of poor weld quality. Though initially attributed to the earthquake, after reinspection it was the judgment of the inspecting engineers that the W1 discontinuities were weld defects which went undetected at the time of construction, rather than earthquake damage (Black and Veatch, unpublished report, 1997). Subsequent research on a larger set of buildings (Paret 2000) reached a similar conclusion regarding the origin of *W*1s in those structures.

Despite the fact that inspections did not reveal any structural damage, the possibility exists that some connection fractures caused by earthquakes up to and including Northridge went undetected because of the low inspection rate, though this rate met FEMA 267 guidelines (FEMA 1995). Inspections meeting these guidelines were intended to detect widespread or severe fracture damage that might pose a safety threat, rather than a small number of isolated fractures.

The base accelerations were approximately twice as large in the Whittier Narrows earthquake compared to the Northridge earthquake. Therefore, it is possible that a few isolated fractures occurred during the Whittier Narrows earthquake, and were not detected immediately afterward (because inspectors were not

Table 2. Modal Frequencies from Fourier Amplitude Spectra

	$N-S$ translation				$E-W$ translation				Torsion			
	Mode 1		Mode 2		Mode 1		Mode 2		Mode 1		Mode 2	
Earthquake	f (Hz)	T (s)	f (Hz)	T (s)	f (Hz)	T (s)	f (Hz)	T (s)	f (Hz)	T (s)	f (Hz)	T (s)
San Fernando	0.49	2.05	1.33	0.75	0.49	2.05	1.41	0.71	—	—	—	—
Point Mugu	0.52	1.91	1.36	0.74	0.51	2.00	1.40	0.71	—	—	—	—
Whittier Narrows	0.51	1.95	1.33	0.75	0.55	1.82	1.46	0.68	—	—	—	—
WN aftershock October 14, 1987	0.51	1.95	1.43	0.70	0.52	1.91	1.22	0.82	—	—	—	—
WN aftershock February 11, 1988	0.54	1.86	1.42	0.71	0.56	1.78	1.51	0.66	—	—	—	—
Upland	0.49	2.02	1.32	0.76	0.51	1.97	1.42	0.70	0.83	1.20	2.20	0.46
Sierra Madre	0.47	2.13	1.35	0.74	0.49	2.02	1.27	0.79	0.82	1.22	2.21	0.45
Landers	0.48	2.10	1.29	0.77	0.48	2.10	1.28	0.78	0.81	1.24	2.12	0.47
Big Bear	0.49	2.05	1.30	0.77	0.49	2.05	1.26	0.79	0.82	1.22	2.29	0.44
Northridge	0.47	2.13	1.28	0.78	0.47	2.13	1.28	0.78	0.79	1.26	2.15	0.47
NR aftershock March 20, 1994	0.51	1.97	1.33	0.75	0.50	2.00	1.33	0.75	0.83	1.20	2.32	0.43
Hector Mine	0.46	2.18	1.29	0.78	0.49	2.02	1.34	0.74	0.79	1.27	2.08	0.48
West Hollywood	0.51	1.97	1.29	0.78	0.51	1.97	1.57	0.64	0.84	1.18	2.33	0.43
Compton	0.57	1.74	1.51	0.66	0.55	1.82	1.60	0.63	0.92	1.09	2.54	0.39
Big Bear City	0.52	1.93	1.40	0.72	0.55	1.82	1.55	0.65	0.89	1.12	2.36	0.42
San Simeon	0.48	2.07	1.23	0.81	0.49	2.05	1.21	0.82	0.79	1.26	2.22	0.45

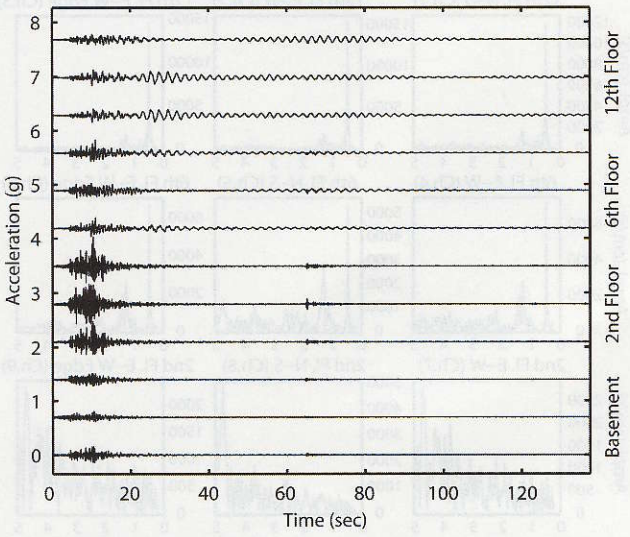

Fig. 3. Acceleration time histories, Northridge earthquake and aftershock at 60 s

looking for fractures at that time), or after the Northridge earthquake (since a relatively small percentage of connections were inspected). Even if undetected fractures occurred, however, it is unlikely that such undetected damage was widespread or severe, due to the inspection program implemented after Northridge.

Analysis of Recorded Building Response

In this paper, analyses of records using frequency domain, joint time–frequency, and system identification methods are presented for the 1994 Northridge earthquake only. However, summaries for the entire data set are provided for maxima of selected horizontal shaking parameters in Table 1, and for modal periods in Table 2. Analyses performed on the remainder of the dataset are discussed in detail in Rodgers et al. (2004).

The response measured at the second floor is significantly different than that measured in the moment-framed stories above, as shown in Fig. 3. The piers between the basement and second story are very stiff despite their height and transfer significant high-frequency energy to the second story. Accelerations at the second floor are significantly larger than those at the 12th floor for sev-

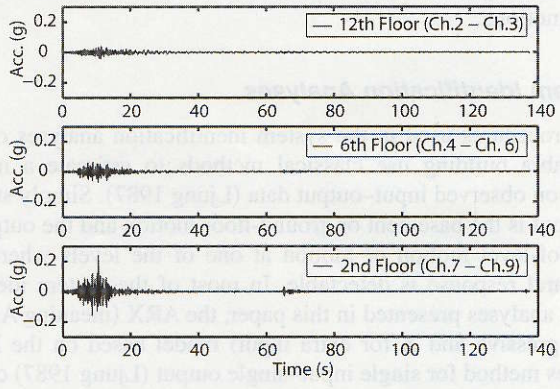

Fig. 4. Torsional accelerations, Northridge earthquake and aftershock at 60 s

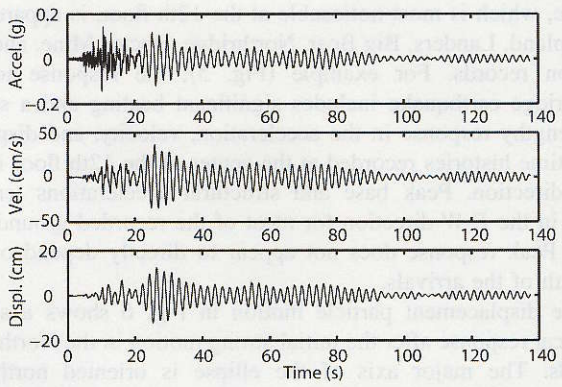

Fig. 5. Acceleration, velocity, and displacement time histories, 12th floor *E-W*, Northridge earthquake

eral records besides Northridge, including Upland, Sierra Madre, and the March 20, 1994 Northridge aftershock. As shown in Fig. 4, during the Northridge earthquake torsional accelerations were significantly larger at the second floor than at other instrumented floors. Second floor accelerations (and torsional accelerations at any level) are unknown for events prior to 1989, when that floor was first instrumented. However, sixth floor translational accelerations were significantly larger than those at the 12th floor during the Whittier Narrows earthquake.

The response of the moment frame above the second floor is characterized by a lengthy response which includes higher modes during the strong shaking portion. Beating in the measured re-

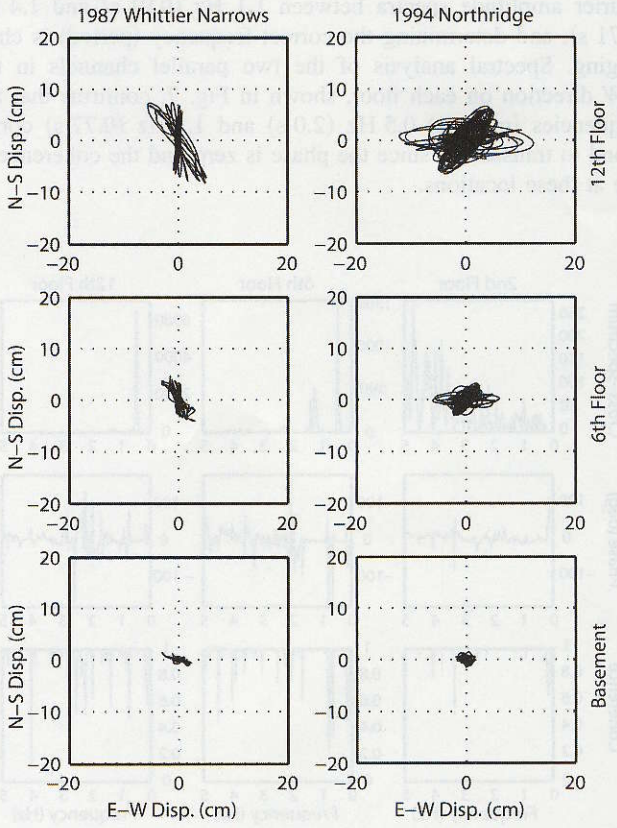

Fig. 6. Particle motion for Whittier Narrows and Northridge earthquakes

sponse, which is most noticeable at the 12th floor, is apparent in the Upland, Landers, Big Bear, Northridge, Hector Mine, and San Simeon records. For example (Fig. 5), the response to the Northridge earthquake includes significant beating and a strong and lengthy response in the acceleration, velocity, and displacement time histories recorded at the center of the 12th floor in the *E-W* direction. Peak base and structural accelerations tend to occur in the *E-W* direction for most of the recorded ground motions. Peak response does not appear to directly depend on the azimuth of the arrivals.

The displacement particle motion in Fig. 6 shows a strong elliptical response after the initial strong motion in the Northridge records. The major axis of the ellipse is oriented northeast-southwest with respect to the building reference coordinates. This response is primarily first mode, and appears to be nearly free vibration as base input motions are small. Little or no torsion was observed during this elliptical response, as shown in Fig. 4, in contrast to the larger torsional response during the strongest shaking. The cause of this response does not appear to be related to a particular earthquake, but is more likely caused by the building's structural characteristics.

Frequency Domain Analyses

First and second mode frequencies are determined from Fourier analysis of 12th floor responses for the two translational directions and torsional motion, and are listed in Table 2. The first translational mode frequencies (periods) are similar for all earthquakes at approximately 0.5 Hz (2.0 s) in both *N-S* and *E-W* directions, a finding which is in agreement with all prior studies. The second translational modes are located in the neighborhood of 1.3 Hz (0.77 s), but several peaks are typically present in the Fourier amplitude spectra between 1.1 Hz (0.91 s) and 1.4 Hz (0.71 s), and determining the correct frequency (period) is challenging. Spectral analysis of the two parallel channels in the *E-W* direction on each floor, shown in Fig. 7, confirms that the frequencies (periods) 0.5 Hz (2.0 s) and 1.3 Hz (0.77 s) correspond to translation, since the phase is zero and the coherence is one at these locations.

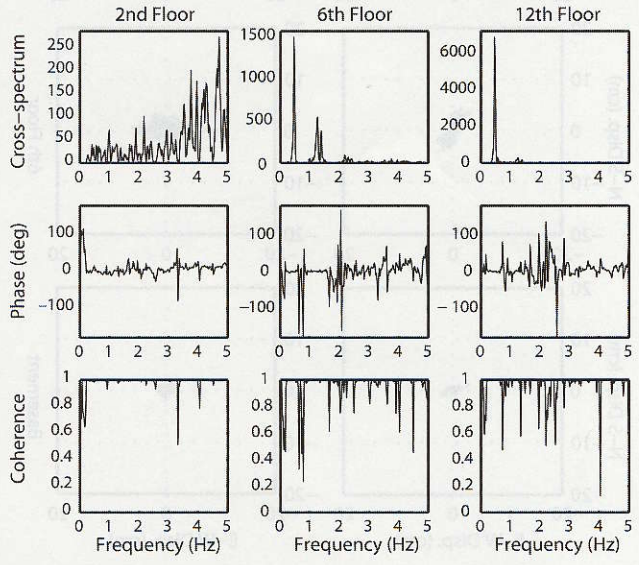

Fig. 7. Spectral analysis of second, sixth, and 12th floors, *E-W* channel pairs, Northridge earthquake

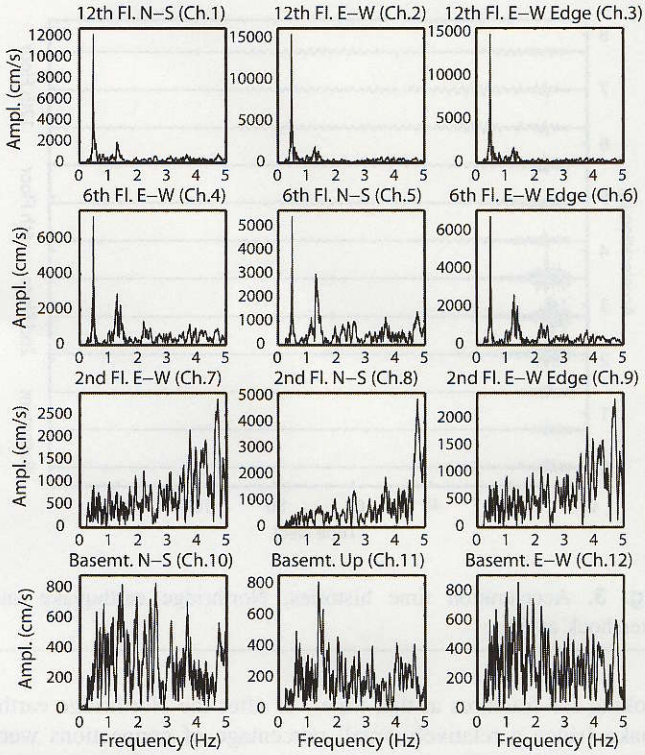

Fig. 8. Fourier amplitude spectra, all channels, Northridge earthquake

The first torsional mode occurs at approximately 0.8 Hz (1.25 s) for all earthquakes, while the second mode occurs in the vicinity of 2.2 Hz (0.45 s). Spectral analysis of the parallel *E-W* channels also indicates torsion at 0.8 Hz (1.25 s) and 2.2 Hz (0.45 s). Spectral analysis of the basement vertical and second and 12th floor horizontal channels also suggest rocking was not a significant contributor to the response.

The difference in the character of the response at the pier tops (second floor) and in the moment frame (sixth and 12th floors) is very noticeable in the Fourier amplitude spectra shown in Fig. 8. The spectra for the basement and second story have significantly higher frequency content than those for the sixth and 12th floors. The transfer of high-frequency energy by the piers is notable in the spectral analyses as well, with basement and second floor motions having significantly greater coherence (particularly at frequencies greater than 5 Hz) than basement and sixth or 12th floor motions.

System Identification Analyses

The procedures used in the system identification analyses of the Alhambra building use classical methods to estimate a model based on observed input–output data (Ljung 1987). Simply stated, the input is the basement or ground-floor motion and the output is the roof-level motion or motion at one of the levels where the structural response is detectable. In most of the system identification analyses presented in this paper, the ARX (meaning AR for autoregressive and X for extra input) model based on the least-squares method for single input–single output (Ljung 1987) coded in commercially available system identification software was used (The MathWorks 1988). The damping ratios are extracted by system identification analyses in accordance with the procedures out-

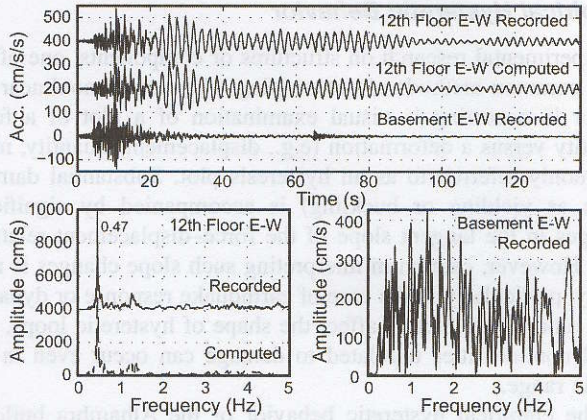

Fig. 9. Results of system identification, East-West direction, Northridge earthquake, and aftershock at 60 s

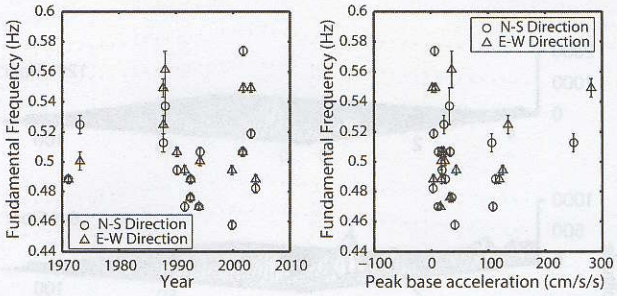

Fig. 10. Variation in first mode period over time (left) and with peak base acceleration (right)

lined by Ghanem and Shinozuka (1995) and Shinozuka and Ghanem (1995). These procedures are demonstratively summarized by Çelebi (1998).

For the Northridge earthquake, a typical result is shown in Fig. 9. Identified natural frequencies are a first mode frequency of 0.47 Hz (2.1 s) in both translational directions, and second mode frequencies of 1.26 Hz (0.79 s) and 1.29 Hz (0.78 s) in the *N-S* and *E-W* directions, respectively. System identification also confirms past observations (Goel and Chopra 1997) of very low damping in the building, determining values of approximately 1.5 and 4% of critical damping in the first and second modes, respectively.

Application of Damage Detection Methods

Several computationally simple damage detection methods are used herein to help ascertain the likelihood that undetected structural damage, particularly moment connection fractures, occurred during the Northridge or prior earthquakes. As discussed previously, a number of more advanced methods were deemed impractical due the low spatial resolution of the instrumentation, building size (>1,000 moment-resisting connections), and building complexity (including the presence of nonstructural components and contents).

Change in Fundamental Frequency

Numerous methods for damage detection have been based on the simple idea that damage reduces the stiffness of the structure and thus causes a decrease in the fundamental vibration frequency. However, this decrease in frequency can also be indicative of nonlinear soil behavior, and lost soil stiffness can be regained over time as the soil recompacts (Luco et al. 1987; Trifunac et al. 2001). Accordingly, care should be exercised in interpreting decreases in fundamental frequency as structural damage. Two methods of examining the frequency response of the structure for changes are examined: (1) simple observation of changes in fundamental frequency (obtained from Fourier amplitude spectra) from one earthquake to the next, and (2) joint–time frequency analysis to detect changes in fundamental frequency during an earthquake.

Changes in Frequencies Extracted from Fourier Amplitude Spectra

Fundamental translational frequencies in both directions are determined for each earthquake and plotted versus earthquake date and base motion amplitude in Fig. 10. The changes in the building's fundamental frequency from the San Fernando earthquake to present show a total variation of approximately 20%, and do not follow a clear trend, except for some short durations which show a gradual decrease in frequency. A clear trend is absent in the amplitude results as well, with large scatter occurring at low amplitudes in particular. In the absence of clear long-term trends, the observed frequency variations should not be interpreted as structural damage despite local variations of approximately 10%, as they likely have other causes (e.g., Luco et al. 1987; Li and Mau 1997; Trifunac et al. 2001). This case illustrates that moderate changes in fundamental frequency between earthquakes should be interpreted with caution, particularly if few records are used, since short-term variations may not be indicative of longer-term trends.

Joint Time-Frequency Analyses

Two analysis techniques falling under the umbrella of joint time–frequency analysis (Black 1998) were employed to determine possible variations in the frequency content of the building response (which might indicate damage) during the Northridge earthquake.

Windowed Discrete-Time Fourier Transform (DTFT)

The windowed discrete-time Fourier transform (also called the moving window fast Fourier transform) was used to evaluate the how the frequency content of the building response varied with time during the Northridge earthquake, and the results are shown graphically in Fig. 11. Observations include: (1) significant higher frequency response (10–25 Hz) occurs in the first 20 s or so of the records, but little thereafter; (2) an aftershock arrival at 60 s is indicated by an increase in higher frequencies; (3) there is no burst of very high frequency energy indicating a fracture; and (4) there is no significant shift in the fundamental frequency during the earthquake. Based on these observations, windowed DTFT analysis does not indicate any structural damage.

Wavelet Analyses

Wavelet analysis involves taking the wavelet transform of a signal using a "mother wavelet" basis function (in contrast to the sine and cosine basis functions used in the Fourier transform). The basics of wavelet analysis are covered in many sources (e.g., Walker 1999) and will not be repeated here. Several mother

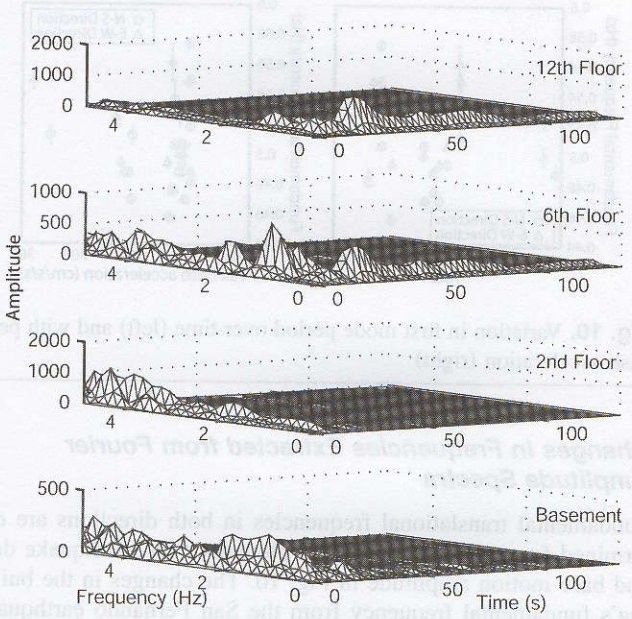

Fig. 11. Variation in frequency response with time determined by windowed DTFT, Northridge earthquake, and aftershock at 60 s

wavelets were used in the analysis of the Alhambra building records (Rodgers et al. 2004), but only results using the Daubechies 4 (Daub4) mother wavelet (see Walker for details) are presented here in the interest of space. The Daub4 wavelet was chosen because of its utility in detecting discontinuous features or changes in signals. The wavelet transform of the Northridge record from the sixth floor *E-W* channel is shown as a spike plot in Fig. 12, with each spike indicating the amplitude of the corresponding wavelet coefficient. Indications of connection fracture would include very large valued wavelet coefficients in the lower scale/higher frequency levels of the spike plot (i.e., dyads −10 to −13 in Fig. 12) indicating sudden changes in the signal or a burst of high-frequency energy (Hou et al. 2000). The wavelet transform of the Northridge response does not show such indications.

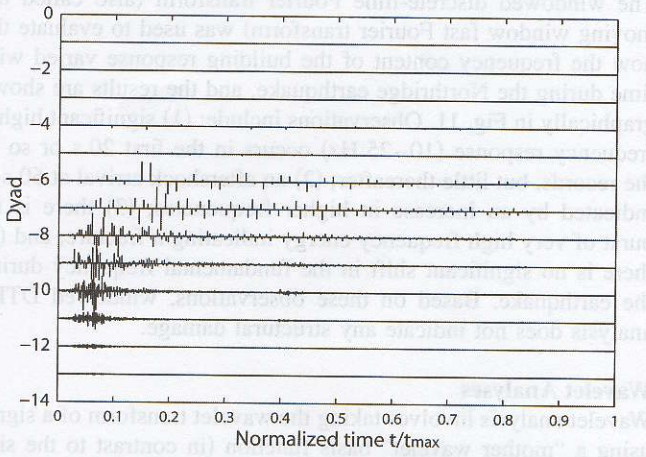

Fig. 12. Wavelet coefficients for sixth floor *E-W*, Northridge earthquake, and aftershock at 0.4 t/t_{max}, Daubechies D4 wavelet

Empirical Hysteretic Behavior

In experimental research on structures or components, one of the most common methods of determining when and if nonlinear behavior is occurring is visual examination of a plot of a force quantity versus a deformation (e.g., displacement) quantity, more commonly referred to as an hysteresis plot. Substantial damage (such as yielding or buckling) is accompanied by significant changes in the tangent slope of the force–displacement relationship. However, caution in interpreting such slope changes is necessary, particularly in the case of earthquake response or dynamic tests, since other factors affect the shape of hysteretic loops, and small nonlinearities unrelated to damage can occur even in the elastic range.

The empirical hysteretic behavior of the Alhambra building was estimated from the recorded accelerations by using displacements computed by the data processors using standard procedures (Stephens and Boore 2004), and by estimating inertia forces. Inertia forces were estimated by multiplying lumped floor masses by the recorded accelerations, with accelerations at the floors without instruments determined by interpolation. Past investigators (De la Llera and Chopra 1998; Goel 2004) have used a procedure that involves interpolation of displacements using cubic splines, followed by double differentiation and low-pass filtering to obtain accelerations. This method was found to be more robust than direct interpolation of accelerations (De la Llera and Chopra 1998), since the displaced shape of the structure is typically continuous and thus better suited to cubic spline interpolation. The sum of the inertia forces provides a good estimate of the base shear forces, since the building has low damping. The base shear–roof displacement hysteresis plot shown in Fig. 13 provides an estimate of the equivalent global stiffness and shows no large excursions with significant changes in tangent stiffness, which suggests that no significant nonlinear behavior occurred.

Presence of High-Frequency, Transient Accelerations

Connection fractures have been observed to cause high-frequency, transient accelerations in shaking table tests of a steel moment frame specimen (Rodgers and Mahin 2006). The possible use of the presence of high-frequency transients to detect fracture damage is examined in a concurrent study (Rodgers and Çelebi 2005), and several observations from that study are included here.

First, transient accelerations in the Northridge record at 65 s (see Fig. 4) are from a well-documented aftershock and are not due to fracture damage. Second, no high-frequency spikes were observed in the uncorrected or corrected accelerations for the Northridge or Whittier Narrow earthquakes. This could mean that: (1) no fractures capable of causing transients occurred (even if W1 indications are earthquake caused, they are not expected to generate transients); or (2) fractures occurred and generated transients, but the transients were not recorded due to instrument limitations or a large distance between the fracture and the instrument. The results from the high-frequency transient method are consistent with those obtained using wavelet analysis.

Conclusions

The seismic instrumentation systems in the Alhambra building have recorded a number of earthquakes since the building was instrumented in 1971, including the building's response to most of the major Southern California earthquakes in that time period. The building's response is characterized by low damping, ex-

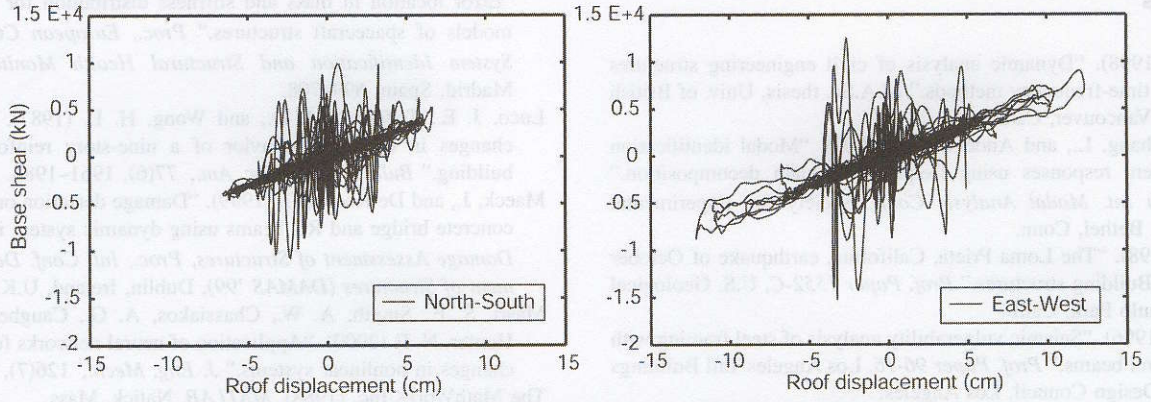

Fig. 13. Empirical hysteretic behavior, Northridge earthquake

tended periods of vibration including an interesting elliptical particle motion, beating, higher accelerations at intermediate stories than at the roof, and significant higher-mode participation and torsion at the second floor during strong shaking. This response is significantly more complex than that expected for a very regular structure. The very stiff concrete piers, which extend to the second floor, cause the response at the second floor to be much more like that of the basement than that of the moment frame above. An elliptical particle motion different from that observed during strong shaking occurs in the moment frame during the periods of extended vibration after the cessation of strong shaking. The cause of this elliptical response has yet to be determined, but it has been observed at different levels of shaking, so is not likely due to the characteristics of a particular earthquake.

After the Northridge earthquake, small weld defects or cracks (FEMA designation W1) were discovered as a result of intrusive inspections. It is probable that these were pre-existing conditions, although it is extremely difficult to determine this conclusively. The simple damage detection methods applied to the structure, including those intended to detect fractures, do not indicate structural damage. This result is consistent with the limited postearthquake inspections conducted after the Northridge earthquake, which found no structural damage (W1s were not considered structural damage) and limited nonstructural damage.

However, this case study demonstrates the occurrence of substantial variations in system vibration properties over time which do not appear to be related to structural damage. Such variability may cause difficulties for many vibration-based damage detection methods. The Alhambra building provides an example of the challenges involved in detecting real building damage using recorded seismic data from a limited number of accelerometers, particularly when the building response is complex. Many of the recently proposed damage detection methods were impractical in this case due to very heavy computational demands, requirements for a detailed and accurate three-dimensional finite element model, and the need for more closely spaced instruments. The density of the conventional instrumentation arrays currently installed in buildings is limited by cost factors. It is anticipated that the development of durable and reliable wireless sensors will be necessary for the deployment of arrays with sufficient density for low levels of damage to be detected and located in large buildings. Temporary deployments of dense arrays using currently available wireless technology are not likely to yield response data from damaging earthquakes, thus limiting their value in damage detection. In the interim, intermediate-density arrays with at least three conventional horizontal sensors at each floor level, although more expensive, have the potential to greatly enhance the utility of the response data for damage detection. Improvements in analysis and computational capabilities for large problems will also be necessary in order to handle the volume of data generated by large sensor networks.

Postearthquake condition assessment from instrumental data could also be significantly improved by the development of reliable methods for displacement measurement and/or computation. Displacement quantities are currently the primary engineering demand parameters used in evaluating the seismic response of buildings, and readily available, accurate displacement response data could significantly improve the quality of rapid postevent condition assessments.

Acknowledgments

The writers gratefully acknowledge the input of the following persons: Chris Stephens and Roy Tam of the USGS National Strong Motion Program Data Center, Ahmet Sanli of Uzun and Case Engineers, Howard Bundock of USGS, Steven Cloke and Michael Cholakian of the Los Angeles County Department of Public Works, Albert Chen of Black and Veatch, Inc., and James Anderson of the University of Southern California.

Notation

The following symbols are used in this paper:

A_{12o} = maximum acceleration measured at 12th floor level;
A_{bo} = maximum acceleration measured at basement level;
A_{so} = maximum acceleration measured in structure, excluding base;
D_{12o} = maximum displacement calculated at 12th floor level;
D_{bo} = maximum displacement calculated at basement level;
F_y = yield stress;
f = frequency;
M = moment magnitude;
T = period; and
ζ = equivalent viscous damping ratio.

References

Black, C. J. (1998). "Dynamic analysis of civil engineering structures using joint time-frequency methods." M.A.Sc. thesis, Univ. of British Columbia, Vancouver, Canada.

Brinker, R., Zhang, L., and Andersen, P. (2000). "Modal identification from ambient responses using frequency domain decomposition." *Proc., 18th Int. Modal Analysis Conf.*, Society for Experimental Mechanics, Bethel, Conn.

Çelebi, M. (1998). "The Loma Prieta, California, earthquake of October 17, 1989—Building structures." *Prof. Paper 1552-C*, U.S. Geological Survey, Menlo Park, Calif.

Cohen, J. M. (1996). "Seismic vulnerability analysis of steel framing with deep spandrel beams." *Prof. Paper 96-16*, Los Angeles Tall Buildings Structural Design Council, Los Angeles.

De la Llera, J. C., and Chopra, A. K. (1998). "Evaluation of seismic code provisions using strong motion building records from the 1994 Northridge earthquake." *Rep. No. UCB/EERC–97/16*, Earthquake Engineering Research Center, Univ. of California, Berkeley, Calif.

Doebling, S. W., and Farrar, C. R. (1997). "Using statistical analysis to enhance modal-based damage identification." *Structural Damage Assessment Using Advanced Signal Processing Procedures, Proc., Int. Conf. Damage Assessment of Struct. (DAMAS '97)*, Univ. of Sheffield, Sheffield, U.K., 199–210.

Dunand, F. (2005). "Pertinence du bruit de fond sismique pour la caractérisation dynamique et l'aide au diagnostic sismique de structures de génie civil." Doctoral dissertation, Univ. Joseph Fourier, Grenoble, France (in French).

Dunand, F., Rodgers, J. E., Acosta, A. V., Salsman, M., Bard, P.-Y., and Çelebi, M. (2004). "Ambient vibration and earthquake strong-motion data sets for selected USGS extensively instrumented buildings." *Open-File Rep. No. 2004-1375*, U.S. Geological Survey, Menlo Park, Calif.

FEMA. (1995). "Interim guidelines, inspection, evaluation, repair, upgrade and design of welded moment resisting steel structures." *FEMA-267*, Prepared by the SAC Joint Venture for the Federal Emergency Management Agency, Washington, D.C.

Fritzen, C. P., and Boehle, K. (1999a). "Identification of damage in large-scale structures by means of measured FRFs—Procedure and applications to the I40 highway bridge." *Damage Assessment of Structures, Proc., Int. Conf. Damage Assessment of Structures (DAMAS '99)*, Dublin, Ireland, U.K., 310–319.

Fritzen, C. P., and Boehle, K. (1999b). "Parameter selection strategies in model-based damage detection." *Proc., Structural Health Monitoring 2000*, Stanford Univ., Stanford, Calif., 901–911.

Ghanem, R., and Shinozuka, M. (1995). "Structural system identification. I: Theory." *J. Eng. Mech.*, 121(2), 255–264.

Goel, R. K. (2004). "Evaluation of nonlinear static procedures using strong-motion building records." *Proc., SMIP04 Seminar*, California Geological Survey, Sacramento, Calif.

Goel, R. K., and Chopra, A. K. (1997). "Vibration properties of buildings determined from recorded earthquake motions." *Rep. No. UCB/EERC–97/14*, Earthquake Engineering Research Center, Univ. of California, Berkeley, Calif.

Hou, Z., Noori, M., and St. Amand, R. (2000). "Wavelet-based approach for structural damage detection." *J. Eng. Mech.*, 126(7), 677–683.

International Conference of Building Officials (ICBO). (1967). *Uniform building code*, Whittier, Calif.

Kim, H., and Melhem, H. (2003). "Damage detection of structures by wavelet analysis." *Eng. Struct.*, 26, 347–362.

Li, Y., and Mau, S. T. (1997). "Learning from recorded earthquake motion of buildings." *J. Struct. Eng.*, 123(1), 62–69.

Ljung, L. (1987). *System identification: Theory for the user*, Prentice–Hall, Upper Saddle River, N.J.

Lopez-Diaz, J., Cuerno-Rejado, C., Luengo, P., and Alexiou, K. (2000). "Error location in mass and stiffness distribution for finite element models of spacecraft structures." *Proc., European COST F3 Conf. System Identification and Structural Health Monitoring*, COST, Madrid, Spain, 699–708.

Luco, J. E., Trifunac, M. D., and Wong, H. L. (1987). "On apparent changes in dynamic behavior of a nine-story reinforced concrete building." *Bull. Seismol. Soc. Am.*, 77(6), 1961–1983.

Maeck, J., and De Roeck, G. (1999). "Damage detection on a prestressed concrete bridge and RC beams using dynamic system identification." *Damage Assessment of Structures, Proc., Int. Conf. Damage Assessment of Structures (DAMAS '99)*, Dublin, Ireland, U.K., 320–327.

Masri, S. F., Smyth, A. W., Chassiakos, A. G., Caughey, T. K., and Hunter, N. F. (2000). "Application of neural networks for detection of changes in nonlinear systems." *J. Eng. Mech.*, 126(7), 666–676.

The MathWorks Inc. (1988). *MATLAB*, Natick, Mass.

Nakamura, M., Masri, S. F., Chassiakos, A. G., and Caughey, T. K. (1998). "A method for non-parametric damage detection through the use of neural networks." *Earthquake Eng. Struct. Dyn.*, 27, 997–1010.

Papadimitriou, C., Levine-West, M., and Milman, M. (1997). "Structural damage detection using modal test data." *Proc., Struct. Health Monitoring, Current Status and Perspectives*, Stanford Univ., Stanford, Calif., 678–689.

Paret, T. F. (2000). "The W1 issue. I: Extent of weld fracturing during Northridge earthquake." *J. Struct. Eng.*, 126(1), 10–18.

Rodgers, J. E., and Çelebi, M. (2005). "A proposed method for the detection of connection fractures in steel moment frames using recorded accelerations." *Open-File Rep. No. 2005-1375*, U.S. Geological Survey, Menlo Park, Calif.

Rodgers, J. E., and Mahin, S. A. (2006). "Effects of connection fractures on global behavior of steel moment frames subjected to earthquakes." *J. Struct. Eng.*, 132(1), 78–88.

Rodgers, J. E., Sanli, A. K., and Çelebi, M. (2004). "Seismic response analysis of a 13-story steel moment-framed building in Alhambra, California." *Open-file Rep. No. 2004-1338*, U.S. Geological Survey, Menlo Park, Calif.

Ruotolo, R., and Surace, C. (1998). "Diagnosis of damage in a steel frame." *Proc., 16th Int. Modal Analysis Conf.*, Society for Experimental Mechanics, Bethel, Conn., 609–615.

Sanli, A. K., and Çelebi, M. (2002). "Earthquake damage detection of a thirteen story building using recorded responses." *Proc., 3rd Int. Workshop on Structural Health Monitoring*, Stanford Univ., Stanford, Calif.

Shinozuka, M., and Ghanem, R. (1995). "Structural system identification. II: Experimental verification." *J. Eng. Mech.*, 121(2), 265–273.

Sohn, H., Farrar, C. R., Hemez, F. M., Shunk, D. D., Stinemates, D. W., and Nadler, B. R. (2003). "A review of structural health monitoring literature: 1996-2001." *Rep. No. LA-13976-MS*, Los Alamos National Laboratory, Los Alamos, N.M.

Stephens, C. D., and Boore, D. M. (2004). "ANSS/NSMP strong-motion record processing and procedures." *Proc., COSMOS Invited Workshop on Record Processing Guidelines*, Consortium of Organizations for Strong Motion Observation Systems, Richmond, Calif.

Stubbs, N., Sikorsky, C., Park, S. C., and Bolton, R. (1999). "Verification of a methodology to nondestructively evaluate the structural properties of bridges." *Proc., Struct. Health Monitoring 2000*, Stanford Univ., Stanford, Calif., 440–449.

Trifunac, M. D., Ivanovic, S. S., and Todorovska, M. I. (2001). "Apparent periods of a building. I: Fourier analysis." *J. Struct. Eng.*, 127(5), 517–526.

Van Overschee, P., and De Moor, B. (1993). "Subspace algorithm for the stochastic identification problem." *Automatica*, 29(3), 649–660.

Walker, J. S. (1999). *A primer on wavelets and their scientific applications*, Chapman & Hall/CRC, Boca Raton, Fla.